NUCLEAR INSTRUMENTS AND METHODS 90 (1970) 207–216; © NORTH-HOLLAND PUBLISHING CO.

NEW CASCADE ANALYSIS TECHNIQUES FOR DETERMINING SPONTANEOUS ATOMIC TRANSITION PROBABILITIES

L. J. CURTIS*, R. M. SCHECTMAN, J. L. KOHL, D. A. CHOJNACKI and D. R. SHOFFSTALL

University of Toledo, Toledo, Ohio, U.S.A.

Several new analysis techniques which account for the effects of cascades in the measurement of atomic transition probabilities have been developed at the University of Toledo, and will be described here. These techniques involve the incorporation of information from the direct measurement of the decay curves of cascading transitions into the analysis of the decay curve of the main level of interest.

The traditional curve fitting techniques, as well as the new analysis techniques, are investigated by the use of computer simulated data containing various numbers of known exponentials. A diagrammatic mnemonic which trivially generates the theoretical decay curves for cascade schemes of arbitrary complexity will be described.

The traditional curve fitting techniques are extended to include constraints imposed by the coefficients in the theoretical decay curve, which can be measured in terms of relative intensities of the cascading transitions.

The population differential equation is converted to an integral equation involving only experimentally measurable quantities and the desired transition probability. Integrals over some arbitrary time interval of the decay curves can be photometrically measured, and given a common normalization through a wavelength relative efficiency calibration of the detection system. Integrated decay curves of all transitions, either directly into or out of the level of interest, can be summed in a manner which determines its transition probability. By varying the choice of time interval it can be verified that all contributing transitions have been correctly included. A variation of this technique allows the construction of the decay curve of an unmeasured cascade, provided the transition probability of the level into which it cascades is known. This variation can be used to investigate radiationless transitions and transitions outside the range of available detectors. Further, if there is additional a priori information concerning the shape of the unseen cascade decay curve, both its lifetime and that of the level into which it cascades can be determined.

1. Introduction

The measurement of atomic transition probabilities has long been complicated by cascade repopulation of the level being studied after its initial excitation. To formulate the problem, consider a set of levels which have some initial population $N_r(0)$. A level n is depopulated by spontaneous transitions to lower levels f, but is repopulated by cascades from higher levels i. The experimentally measured quantity is the intensity of light emitted in the transition, and is given (in photons/sec) by

$$I_{nf}(t) = N_n(t) A_{nf}, \tag{1}$$

where A_{nf} is the spontaneous transition probability which we wish to determine. The sole time dependence of the intensity resides in the population of the decaying level, so that all transitions from the same upper level will have the same shape as a function of time. Thus, relative transition probabilities (branching ratios) can be obtained from ratios of intensities of transitions from the same upper level measured at the same point in time, or at some equilibrium population. In order to determine absolute transition probabilities, it is necessary to consider the level population, which is governed by the differential equation

$$\mathrm{d}N_n/\mathrm{d}t = \sum_{i=n+1}^{m} N_i(t) A_{in} - N_n(t) \sum_{f=1}^{n-1} A_{nf}. \tag{2}$$

This equation includes the effects of cascades and spontaneous emission, but neglects effects such as stimulated emission, absorption, and collisional deexcitation. The lifetime of a level τ_j is the e-folding time which would exist if there were no cascades, and its inverse, the decay constant α_j, is the sum of transition probabilities taken over exit channels, thus

$$1/\tau_j = \alpha_j = \sum_{f=1}^{j-1} A_{jf}. \tag{3}$$

2. Polarization and cascading

In addition to compounding exponential dependences, cascades can introduce more subtle difficulties if polarization is present. Since the intensity is usually experimentally sampled within some small solid angle, one must exert care that there are no time dependent geometric factors which alter the proportionality between the light sampled and the total light emitted into all 4π sterad. This can occur if degenerate substates are not statistically populated, but have a preferred direction inherent in the excitation, such as the beam axis[1]). Cascade repopulation may then wash out this initial sample polarization as a function of time, hence washing out the asymmetry in the angular distribution and in the direction of the electric field vector of the emitted radiation. Thus, apparent time variations in the intensity can arise through a misinterpretation of the radiation pattern. The angular distribution of

* Presented the paper.

emitted radiation for a polarized sample is given by

$$\frac{dI_{ij}}{d\Omega}(\theta,t)=\frac{I_{ij}(t)}{4\pi}\left[\frac{1-P_{ij}(t)\cos^2\theta}{1-P_{ij}(t)/3}\right], \quad (4)$$

where

$$P_{ij}(t)=\frac{I_{ij}^{\parallel}(t)-I_{ij}^{\perp}(t)}{I_{ij}^{\parallel}(t)+I_{ij}^{\perp}(t)} \quad (5)$$

and $I_{ij}^{\parallel}(t)$ and $I_{ij}^{\perp}(t)$ are the intensities measured at 90° to the axis of polarization through polarizing filters oriented parallel and perpendicular to the axis of polarization.

This angular distribution is plotted in fig. 1 for various values of the polarization. Notice that for a sample of polarization $P=+1$, viewed at 90°, washout to isotropy causes a 33% change in intensity, from 1.5 to 1.0, with no change in the total integrated intensity. Further, variations in detection efficiencies for light of differing polarizations can lead to similar apparent intensity variations during a cascade washout of polarization.

We have made preliminary measurements through polarizing filters aligned parallel and perpendicular to a pulsed electron beam source, and obtained decay curves differing by 15%. Since instrumental polarizations are time independent, this implies a cascade washout of an initial polarization, which could lead to an erroneous lifetime determination.

The cascade analysis techniques which will be described below will neglect polarization effects, but could, with slight modification, be adapted to include such effects.

3. Threshold measurements

The cascade problem could be circumvented through threshold excitation of the sample, exciting no levels above the level of interest. This technique has a number of drawbacks. For one thing, energy regulation is difficult at tens of electron volts. In addition, excitation cross sections for the level of interest become vanishingly small near threshold, reducing measured light outputs. Further, polarization effects may be more pronounced near threshold. Finally, threshold excitation is not feasible for ionized atomic spectroscopy studies such as those of beam foil, and cascade effects must be accounted for.

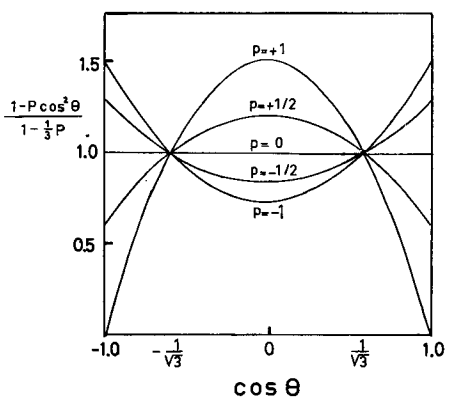

Fig. 1. Angular distribution of radiation as a function of polarization.

4. Curve fitting techniques

In many cases curve fitting of decay curves to exponential forms is a quite satisfactory method of analysis. Further, urgent requirements for approximate lifetimes have often led to the acceptance of some inaccuracy, and allowed wider use of curve fitting. Fits to forms including more than two exponentials are usually not reliable, but there are often cases where one and two exponential forms are appropriate. Cascades become negligible if their lifetimes are either extremely long or extremely short compared to the transitions of interest, and a single exponential, analytically-determined fit can be made to the data. If the cascades have lifetimes reasonably different from that of the transition of interest they can often be included as a single effective exponential and a two-exponential fit can be made. A two-exponential fit is not analytically determinable but can be made by a search routine such as the Method of Steepest Descent, the Gauss-Seidel Method, or appropriate Monte Carlo Methods. Such a fit is shown in fig. 2.

5. Exponential forms

The exact time dependence of a cascade level scheme contains many exponentials. A sample decay scheme is shown in fig. 3. In addition to the exponential term for the transition of interest, there is also one exponential term for each level which cascades either directly or indirectly into the level of interest. (Clearly some of the transitions indicated on the sample scheme will be forbidden by selection rules, but indirect cascading will still contribute exponential terms.) These exponential forms are easily determinable. We have shown, through an iteration of the differential equation and an exchange of sum and integrals, the integrals can be exactly performed to arbitrary order[2]). This allows an interpretation in terms of a diagrammatic decomposition, where cascades of various orders can be considered separately and the exponential dependence written as a sum of canonical forms, as shown in fig. 4.

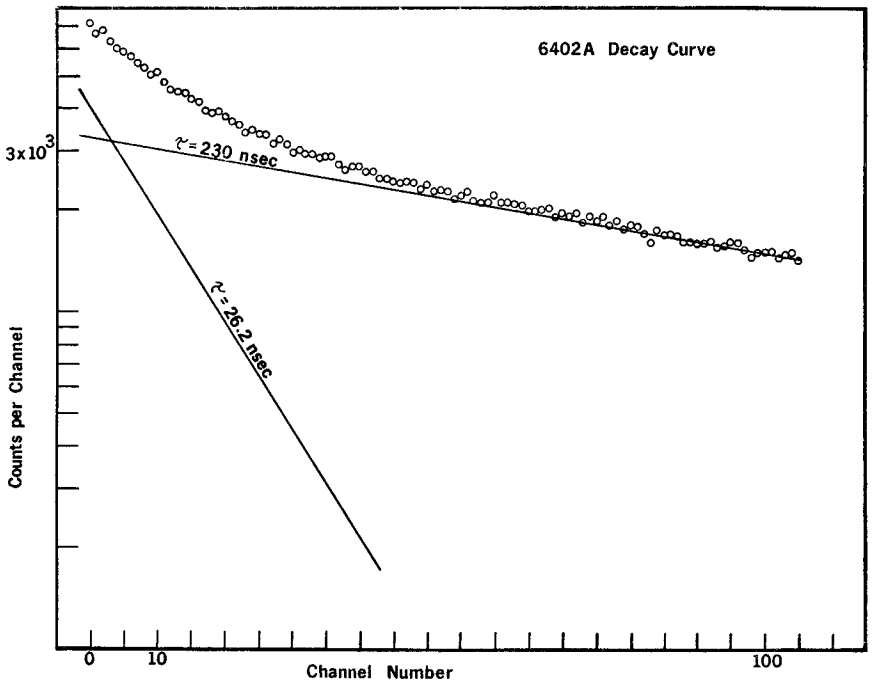

Fig. 2. Two-exponential fit to experimental data.

A sample calculation is shown in fig. 5. The similarity between various first order cascades and various second order cascades infers the form of cascades of higher order, and one can trivially write out the exponential dependence of a cascade scheme of arbitrary complexity.

6. Simulation of data not amenable to fitting

Using these multi-exponential forms we have constructed simulated data which are not amenable to curve fitting techniques, and sought to test other techniques by which it might be analyzed. A computer simulated three-exponential curve, blending levels of lifetimes 20, 80, and 200 ns, with initial population ratios of 1:2:2.5 is shown in fig. 6. Statistical errors of nominally 1% (but varying, as intensity decreases with time) have been introduced. Timing errors can also be important, but have not been included here. A two-exponential fit, using the computer program "Gausshaus" (modified for exponentials by H. G. Berry), to this three-exponential data is shown on fig. 7. The χ^2 probability indicates a 97% goodness of fit, but the values obtained are a high estimate of the shortest lifetime and a low estimate of the longest lifetime. We repeated this with statistics of 1/10th%, which are much better than are usually obtained experimentally, and were able to obtain a χ^2 probability which indicated we had chosen the wrong functional form, but with the same errors in lifetimes. If the statistics were reduced to 10%, a one-exponential fit and a two-exponential fit differed little in χ^2 probability. Fig. 8 shows a three-exponential fit to the 1% simulated data. Notice that χ^2 probability is slightly improved but the

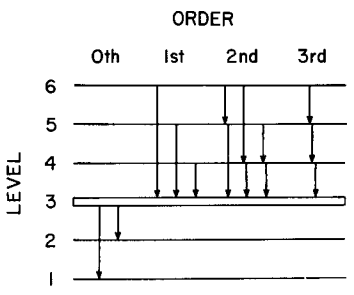

Fig. 3. Sample decay scheme.

$$N_n(t) = N_n(0)e^{-\alpha_n t} + \sum_{i=n+1}^{m} \{\; \overset{i}{\underset{n}{\top\!\!\top}} \;\} + \sum_{i=n+1}^{m-1} \sum_{j=i+1}^{m} \{\; \overset{j}{\underset{i}{\top\!\!\top}} \;\}_n$$

$$+ \sum_{i=n+1}^{m-2} \sum_{j=i+1}^{m-1} \sum_{k=j+1}^{m} \left\{ \begin{array}{c} k \\ j \\ i \\ \hline \\ n \end{array} \right\} + \cdots + \left\{ \begin{array}{c} m \\ \text{m-n steps} \\ \hline \\ n \end{array} \right\}$$

Fig. 4. Diagrammatic cascade decomposition of a level population.

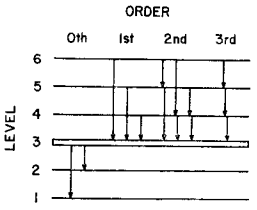

$$N_3(t) = N_3(0)\exp(-\alpha_3 t) + \{6\to3\} + \{5\to3\} + \{4\to3\} + \{6\to5\to3\} + \{6\to4\to3\} + \{5\to4\to3\} + \{6\to5\to4\to3\}$$

$$N_3(t) = N_3(0)\exp(-\alpha_3 t) + N_6(0)A_{63}\left[\frac{\exp(-\alpha_6 t)}{(\alpha_3-\alpha_6)} + \frac{\exp(-\alpha_3 t)}{(\alpha_6-\alpha_3)}\right]$$

$$+N_5(0)A_{53}\left[\frac{\exp(-\alpha_5 t)}{(\alpha_3-\alpha_5)} + \frac{\exp(-\alpha_3 t)}{(\alpha_5-\alpha_3)}\right] + N_4(0)A_{43}\left[\frac{\exp(-\alpha_4 t)}{(\alpha_3-\alpha_4)} + \frac{\exp(-\alpha_3 t)}{(\alpha_4-\alpha_3)}\right]$$

$$+N_6(0)A_{65}A_{53}\left[\frac{\exp(-\alpha_6 t)}{(\alpha_5-\alpha_6)(\alpha_3-\alpha_6)} + \frac{\exp(-\alpha_5 t)}{(\alpha_6-\alpha_5)(\alpha_3-\alpha_5)} + \frac{\exp(-\alpha_3 t)}{(\alpha_6-\alpha_3)(\alpha_5-\alpha_3)}\right]$$

$$+N_6(0)A_{64}A_{43}\left[\frac{\exp(-\alpha_6 t)}{(\alpha_4-\alpha_6)(\alpha_3-\alpha_6)} + \frac{\exp(-\alpha_4 t)}{(\alpha_6-\alpha_4)(\alpha_3-\alpha_4)} + \frac{\exp(-\alpha_3 t)}{(\alpha_6-\alpha_3)(\alpha_4-\alpha_3)}\right]$$

$$+N_5(0)A_{54}A_{43}\left[\frac{\exp(-\alpha_5 t)}{(\alpha_4-\alpha_5)(\alpha_3-\alpha_5)} + \frac{\exp(-\alpha_4 t)}{(\alpha_5-\alpha_4)(\alpha_3-\alpha_4)} + \frac{\exp(-\alpha_3 t)}{(\alpha_5-\alpha_3)(\alpha_4-\alpha_3)}\right]$$

$$+N_6(0)A_{65}A_{54}A_{43}\left[\frac{\exp(-\alpha_6 t)}{(\alpha_5-\alpha_6)(\alpha_4-\alpha_6)(\alpha_3-\alpha_6)} + \frac{\exp(-\alpha_5 t)}{(\alpha_6-\alpha_5)(\alpha_4-\alpha_5)(\alpha_3-\alpha_5)}\right.$$

$$\left. + \frac{\exp(-\alpha_4 t)}{(\alpha_6-\alpha_4)(\alpha_5-\alpha_4)(\alpha_3-\alpha_4)} + \frac{\exp(-\alpha_3 t)}{(\alpha_6-\alpha_3)(\alpha_5-\alpha_3)(\alpha_4-\alpha_3)}\right]$$

Fig. 5. Sample calculation, using diagrammatic mnemonic.

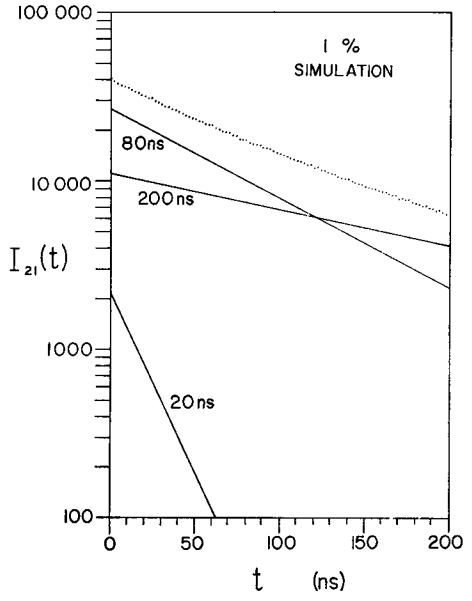

Fig. 6. Blend of levels of 20, 80 and 200 ns lifetimes with initial intensity ratios of 1:2:2.5 with nominally 1% statistical errors simulated.

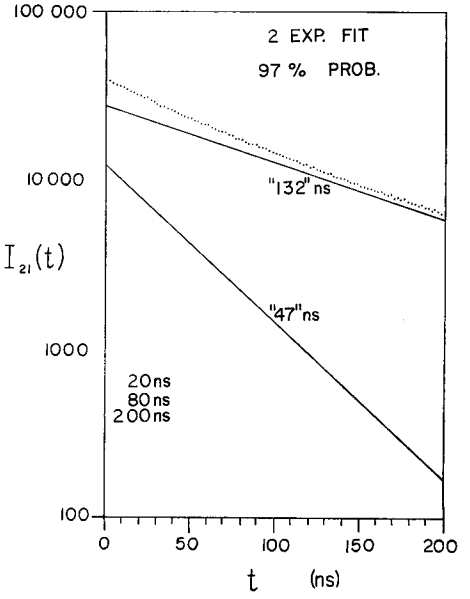

Fig. 7. Two-exponential fit to 3-exponential simulation.

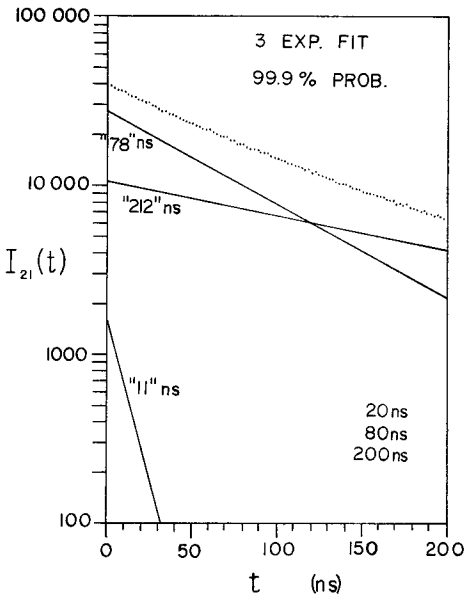

Fig. 8. Three-exponential fit to 3-exponential simulation.

lifetime sought is wrong by a factor of 2, being 11 ns rather than 20 ns. Better statistics give the same χ^2 probability and improve the lifetime only slightly. The 10% statistical data is shown in fig. 9, and a three-exponential fit, given the correct initial values, diverges to a better χ^2 with lifetime values off by factors of 3. These results are summarized in table 1. Let us now consider alternative methods to this exponential fitting technique, which may enable us to analyze this example which was not correctly analyzed by curve fitting.

7. Constrained fits

The number of parameters involved in most exponential fits is twice the number of exponential terms, since it includes one coefficient and one lifetime for each exponential term. As we have seen, the coefficient actually contains measurable quantities and lifetimes, if the cascade scheme is known and if the cascade wavelengths are in a region accessible to detection equipment. If indirect cascades are neglected, the intensity of a transition can be written

$$I_{21}(t_j = \left[I_{21}(0) - \sum_{i=3}^{m} \frac{BI_{i2}(0)\alpha_2}{\alpha_2 - \alpha_i} \right] e^{-\alpha_2 t} + \sum_{i=3}^{m} \frac{BI_{i2}(0)\alpha_2}{\alpha_2 - \alpha_i} e^{-\alpha_i t}, \quad (6)$$

where B is the ratio of the transition probability to the decay constant, if other lower states exist. It can be determined from measured or theoretical branching ratios (or left as free parameter).

$$B = A_{21}/\alpha_2. \quad (7)$$

If one has a relative wavelength calibration[3]), the initial cascade intensities occurring in this equation can be measured, halving the number of free parameters. For a three-exponential direct-cascade scheme, the intensity is

$$I_{21}(t) = \left[I_{21}(0) - \frac{BI_{32}(0)\alpha_2}{\alpha_2 - \alpha_3} - \frac{BI_{42}(0)\alpha_2}{\alpha_2 - \alpha_4} \right] e^{-\alpha_2 t} + \left[\frac{BI_{32}(0)\alpha_2}{\alpha_2 - \alpha_3} \right] e^{-\alpha_3 t} + \left[\frac{BI_{42}(0)\alpha_2}{\alpha_2 - \alpha_4} \right] e^{-\alpha_4 t}. \quad (8)$$

If $I_{21}(t)$, $I_{32}(0)$, and $I_{42}(0)$ are all measurable, the three-exponential case becomes a three-parameter rather than a six-parameter fit. Unfortunately, this determination is greatly complicated if indirect cascades occur, since their initial intensities are also required. However, this method can be applied to a two-exponential fit to reduce the number of parameters from four to two without this problem, since there can be no indirect cascading with a single higher level. The intensity is then given by

$$I_{21}(t) = \left[I_{21}(0) - \frac{BI_{32}(0)\alpha_2}{\alpha_2 - \alpha_3} \right] e^{-\alpha_2 t} + \left[\frac{BI_{32}(0)\alpha_2}{\alpha_2 - \alpha_3} \right] e^{-\alpha_3 t}. \quad (9)$$

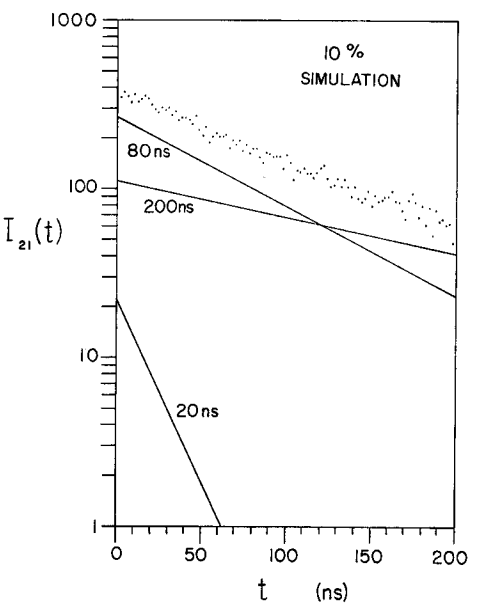

Fig. 9. Blend with nominally 10% statistical errors simulated.

TABLE 1
Fits to simulated data ($\tau_2 = 20$ ns).

Fit	10% Stat. "τ"$_2$	10% Stat. χ^2 prob	1% Stat. "τ"$_2$	1% Stat. χ^2 prob	1/10% Stat. "τ"$_2$	1/10% Stat. χ^2 prob
1 exp	105.4 ns	40%	–	–	–	–
2 exp	64.4 ns	53%	47.0 ns	97%	46.5 ns	0.2%
3 exp	53.0 ns	46%	11.3 ns	99.9%	16.6 ns	99.9%

This technique can often improve the χ^2 probability by reducing the number of degrees of freedom. In addition, we have found that we can separate two exponentials differing only slightly in lifetime by use of the constrained fit. A simulated blend of a 20 ns and a 30 ns lifetime with 10% statistics was correctly analyzed by the two-parameter constrained fit, while a four-parameter fit saw two identical lifetimes, incorrectly indicating a single lifetime somewhere between 20 and 30 ns.

If the intensities of the cascades are sufficient to follow the decay curves as a function of time, their lifetimes can also be determined, further reducing the number of free parameters. However, higher order cascading complicates this type of analysis, and it is possible to use another technique which incorporates the cascade decay curves correctly, without the need for measuring higher order cascades.

8. Analysis by decay curve integration

If a relative wavelength calibration is available and it is possible to measure all direct cascade decay curves, the transition probabilities can be determined by integrating the decay curves[4]). To see this let us rewrite the population equation in terms of intensities. Combining eq. (1) with eq. (2), we obtain

$$\frac{\mathrm{d}I_{nj}/\mathrm{d}t}{A_{nj}} = \sum_{i=n+1}^{m} I_{in}(t) - \sum_{f=1}^{n-1} I_{nf}(t). \tag{10}$$

If we integrate both sides of the equation, and exchange the orders of summation and integration, we obtain

$$[I_{nf}(T) - I_{nj}(0)]/A_{nj} = \sum_{i=n+1}^{m} \int_0^T \mathrm{d}t I_{in}(t) - \sum_{f=1}^{n-1} \int_0^T \mathrm{d}t I_{nf}(t). \tag{11}$$

Solving for A_{ij} we obtain

$$A_{nj} = \frac{I_{nj}(T) - I_{nj}(0)}{\sum_i C_i - \sum_f D_f}, \tag{12}$$

where

$$C_i = \int_0^T \mathrm{d}t I_{in}(t), \tag{13}$$

$$D_f = \int_0^T \mathrm{d}t I_{nf}(t), \tag{14}$$

are experimentally measurable quantities, and correspond to the total light output, integrated over some increment of time, for the cascade and down-transition decay curves. The interpretation is shown in fig. 10. The transition probabilities are thus determined by a time averaged balance of the entrance and exit radiation, irrespective of their individual time dependences, and the initial and final intensities of the level of interest. Experimentally the integrals are easily performed by the electronic logic of a multi-channel analyzer.

There are a number of notable features of this analysis technique. Notice that only direct cascades are involved, with higher order indirect cascading being included by virtue of the shape of the direct cascade

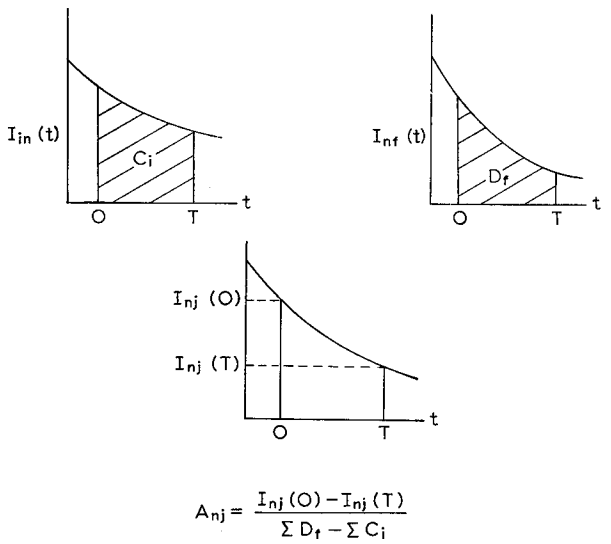

Fig. 10. Experimental interpretation of intensity integrals.

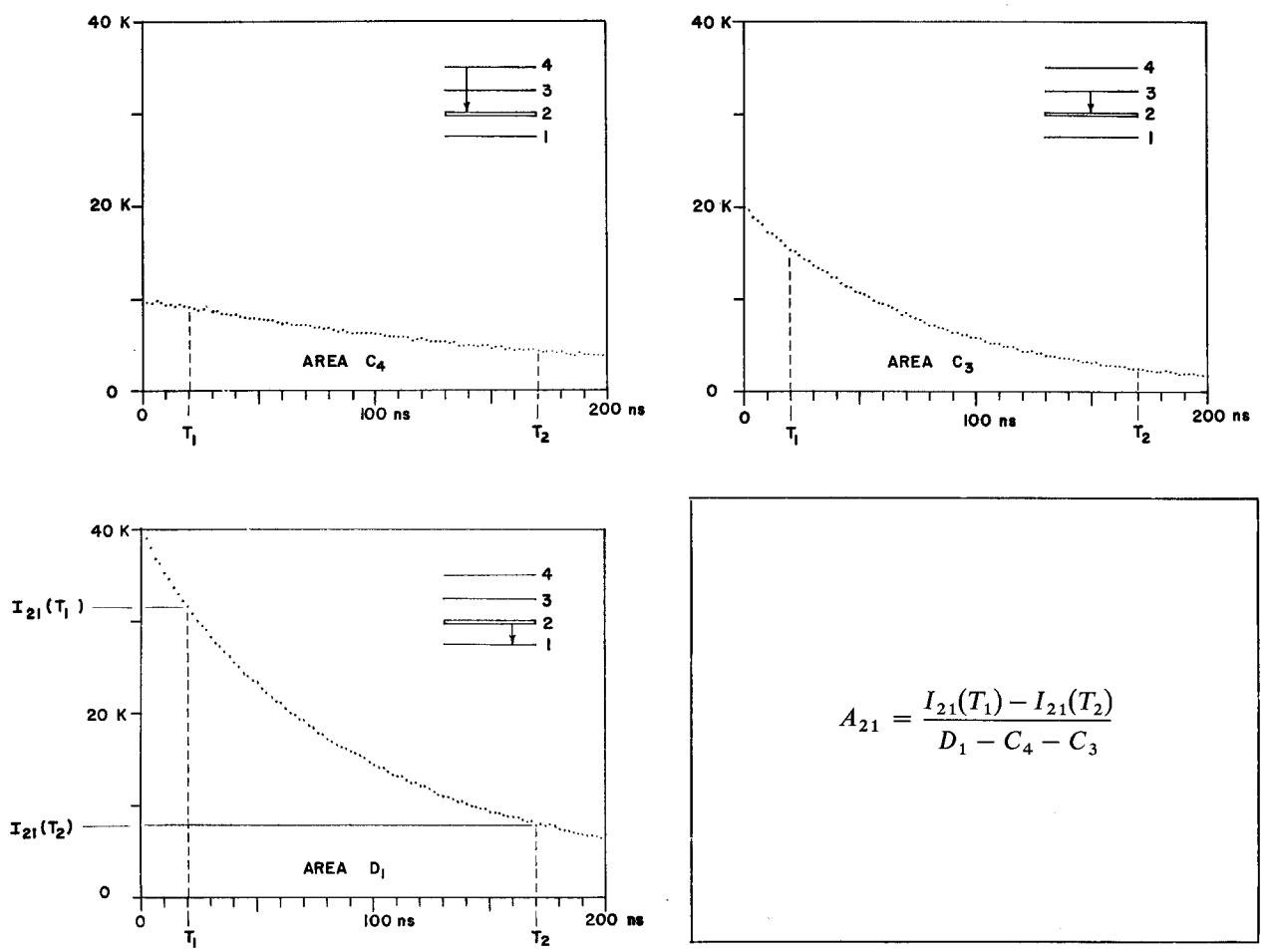

Fig. 11. Analysis of simulated data by decay curve integration.

decay curve. Notice also that a good relative wavelength calibration is essential, so that all integrals have a common normalization and can be added. Also notice that overlapping or unresolvable lines which both cascade directly into the level of interest can be summed simply by widening the spectrometer slit, since only sums of integrals are required. However, also notice that one must measure *all* of the direct cascades – an erroneous result will occur if even one is omitted. Fortunately there is a simple alarm mechanism to check for this. If one varies the integration range and obtains the same transition probability using many different areas under the curves, a consistent result will be obtained only if all cascades have been included. Fig. 11 shows this type of cascade analysis applied to the 1% three-exponential simulation shown earlier. (A perfect wavelength calibration was assumed, although such errors in the normalization of various decay curves could also have been simulated.) Since indirect cascades do not enter, the scheme can be considered as two input channels and one output channel. The areas under intensity curves (4,2) and (3,2) are subtracted from that under intensity curve (2,1), and the transition probability is determined as shown. This calculation yields the correct answer of 20 ns ($\pm$ a few percent) for any integration range of width greater than 50 ns, verifying that no levels have been missed. Surprisingly, when this analysis is applied to the 10% data, which diverged from the correct values for a better fit, the correct value of 20 ns is again obtained for any reasonable range of integration. Thus the incorporation of cascade decay curves into the analysis of the decay curves of the level of interest can markedly improve the accuracy of measurements.

This new analysis technique can also be utilized in several variations for appropriate situations. As one variation, suppose some cascade is not measurable, but another transition from the same upper level is mea-

surable. Both decay curves have the same shape in time, so if good experimental or theoretical branching ratios are available, the desired decay curve can be obtained from the measurable decay curve through an appropriate normalization. As another variation, suppose some transition is totally unmeasurable, but the down transition probability is known. The process can be inverted to generate the decay curve of the unseen transition. This allows one to study transitions outside the range of existing detectors, as well as transitions which proceed by some radiationless process. As a further variation, if there is some a priori information about the unseen transition (perhaps gained through a study of another transition from the same upper level, or some knowledge of populations contributing to second order cascades) it is possible to determine both the decay curve of the missing transition and the transition probability of the down-transition. Specifically, if the missing transition were known to be single exponential in form, one could vary the lifetime of the down-transition and seek the minimum value of χ^2 on the fit of the reconstructed missing decay curve to a single exponential. The three-exponential simulation example was analyzed this way, as is shown in fig. 12. Minimum χ^2 implies a 19.1 ± 1 ns down lifetime, and correctly recoups the missing transition decay curve, as well as its 200 ns lifetime.

9. Application of the new techniques

This new analysis technique has been applied to a measurement of the lifetime of the $2p_9$ level in neon using pulsed electron beam excitation[5]). A simple two-exponential four-parameter fit of the decay curve yielded 26.2 ns (see fig. 2), much longer than some reported results near threshold[6,7]). To apply the new methods, we must consider the level scheme. The $2p_9$ level can decay only into the $1s_5$ level, with wavelength 6402 Å. The direct cascades of significant intensity include eleven transitions with wavelength between 4712 Å and 8377 Å, and one transition of wavelength 11 180 Å. The decay curves of the down transition and all cascades except the 11 180 Å (which was far beyond the infra-red cutoff of the detector employed) were measured.

As a first attempt, the unseen 11 180 Å transition was neglected, and an attempt was made to determine the $2p_9$ lifetime. The aforementioned alarm mechanism told us this missing transition could not be ignored, as a different apparent lifetime was obtained for each choice of range of time integration. We therefore inverted the process, and used a lifetime of 19.4 ns, obtained in a threshold measurement by Bennett and Kindlemann[6]), and generated the unseen decay curve of the 11 180 Å transition. The curve was consistent with being a single exponential of lifetime 195 ± 9 ns, and is shown in fig. 13.

As another check, all eleven measured cascades and the reconstructed unseen cascade were fit to one or two exponentials, giving an initial intensity and a lifetime for each cascade. Curve fitting errors in the cascades

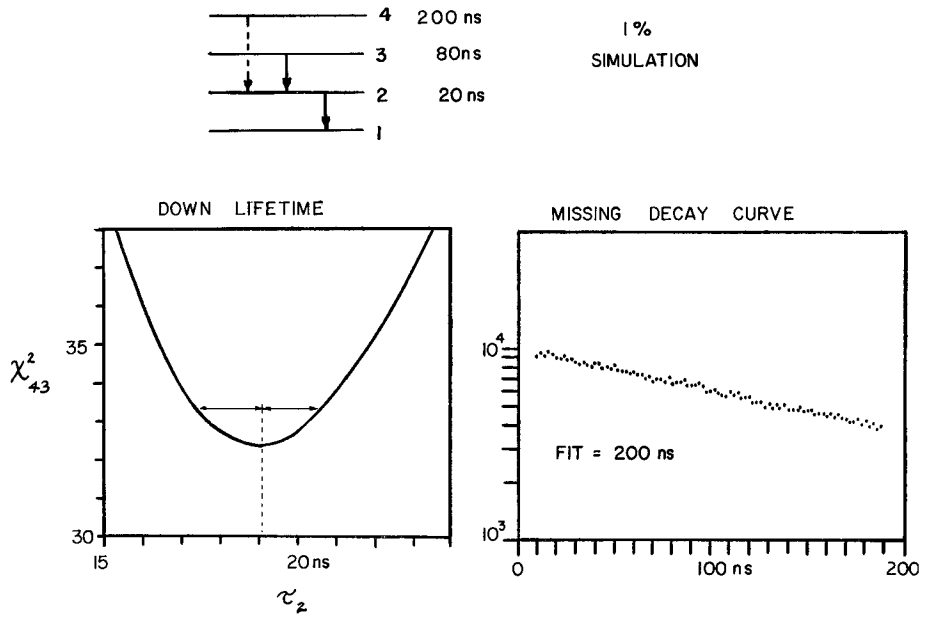

Fig. 12. Simultaneous determination of an unseen cascade decay curve and the down transition probability.

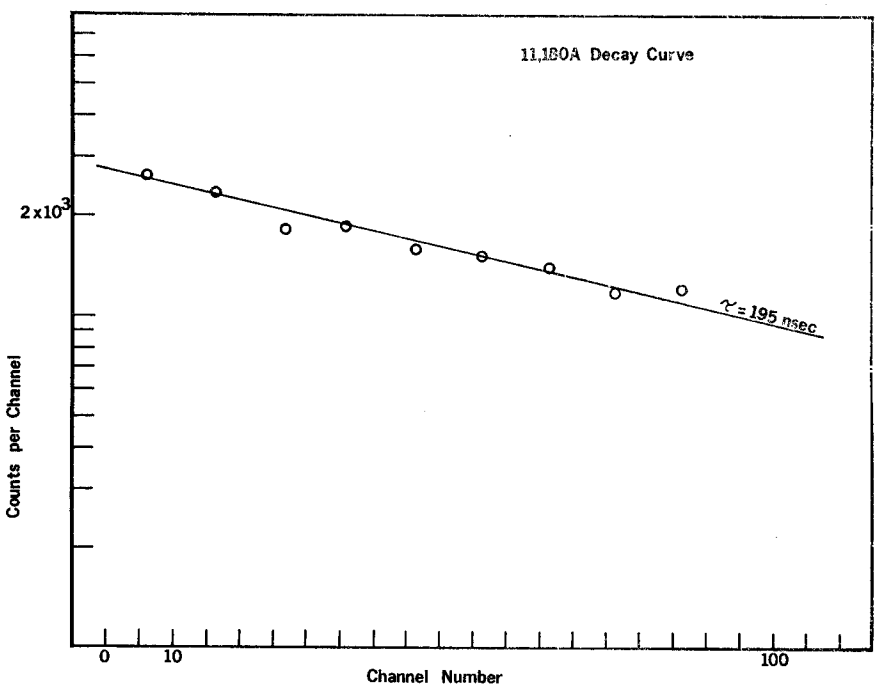

Fig. 13. Reconstruction of the unseen 11 180 Å decay curve.

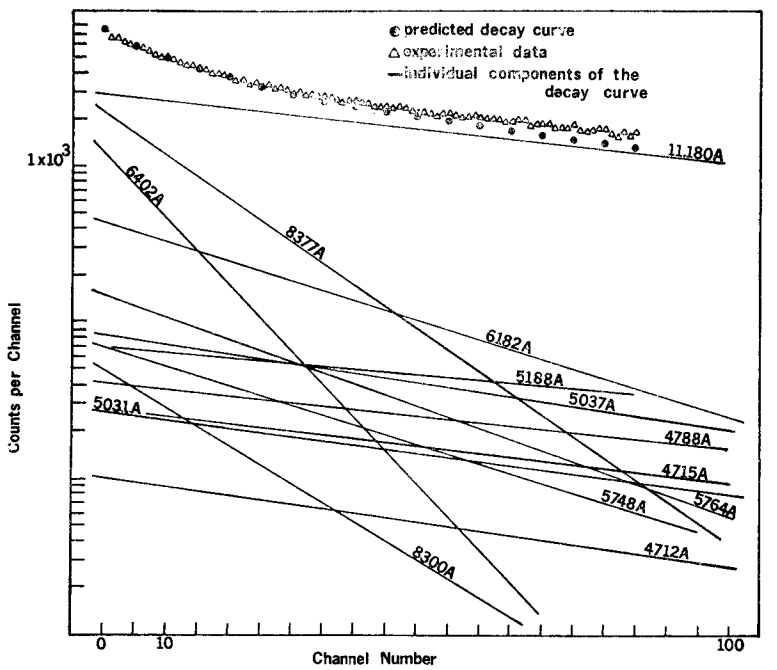

Fig. 14. Blend of the individual components of the intensity decay curve of the 6402 Å emission.

should have a less drastic effect than curve fitting errors in the transition being studied, and if indirect cascades are neglected, eq. (6) can be used (with Bennett and Kindlemann's lifetime and the initial intensity of the down-transition) to form a blend of 13 exponentials, which should approximate the measured $2p_9$ decay curve. This blend, together with the measured curve, is shown in fig. 14. Agreement is quite good at short times, becoming somewhat worse at longer times due to the influence of higher order cascades. A slightly better fit can be obtained by adding a flat background as an empirical correction for higher order cascading.

Since the 11180 Å decay curve seemed to be a single exponential, we investigated the consequences of assuming it to be rigorously a single exponential, and varied the $2p_9$ lifetime so as to give the best χ^2 probability for the 11180 Å fit to a single exponential. We found that the lifetime of the 11180 Å transition was relatively insensitive to this variation, but that the best fit was obtained with a $2p_9$ lifetime of 22 ± 1 ns, which is lower than we obtained by direct curve fitting, and is also more nearly in agreement with the 19.4 ± 0.6 threshold measurement of Bennett and Kindlemann[6]), as well as a 22.5 ± 3.1 ns measurement near threshold by Klose[7]). We have also introduced the empirical flat background as a free parameter to correct for indirect cascading, and found a better χ^2 for slightly lower values of the $2p_9$ lifetime. At present, we are applying these methods to a number of other levels and cascade schemes.

In conclusion, there is a great deal of information in the decay curves of cascades which bears on the analysis of the decay curve of the level of interest. Detailed studies using the methods outlined should permit greater accuracy and reliability in the measurement of atomic transition probabilities.

Note added in proof: Some authors now reserve the word *blend* to denote an unresolved spectral multiplet, for which exponential coefficients correspond directly to initial intensities. As it occurs in this paper, the word *blend* refers to cascaded levels, for which increased resolution does not reduce exponential multiplicity.

References

[1]) B. L. Moiseiwitsch and S. J. Smith, Rev. Mod. Phys. **40** (1968) 238, with Erratum **41** (1969) 574.
[2]) L. J. Curtis, Am. J. Phys. **36** (1968) 1123.
[3]) J. L. Kohl, L. J. Curtis, D. A. Chojnacki and R. M. Schectman, Appl. Opt., to be published.
[4]) J. L. Kohl, Phys. Letters **24A** (1967) 125.
[5]) J. L. Kohl, Ph. D. Thesis (University of Toledo, 1969).
[6]) W. R. Bennett, Jr. and P. J. Kindlemann, Phys. Rev. **149** (1966) 38.
[7]) J. Z. Klose, Phys. Rev. **141** (1966) 181.